Journal of Biomechanics 48 (2015) 2990–2997

Contents lists available at ScienceDirect

Journal of Biomechanics

journal homepage: www.elsevier.com/locate/jbiomech
www.JBiomech.com

Feasible muscle activation ranges based on inverse dynamics analyses of human walking

Cole S. Simpson [a], M. Hongchul Sohn [a], Jessica L. Allen [b], Lena H. Ting [a,b,*]

[a] George W. Woodruff School of Mechanical Engineering, Georgia Institute of Technology, GA, United States
[b] Wallace H. Coulter Department of Biomedical Engineering, Georgia Institute of Technology and Emory University, GA, United States

ARTICLE INFO

Article history:
Accepted 30 July 2015

Keywords:
Motor control
Musculoskeletal model
Muscle coordination
Biomechanics
Gait

ABSTRACT

Although it is possible to produce the same movement using an infinite number of different muscle activation patterns owing to musculoskeletal redundancy, the degree to which observed variations in muscle activity can deviate from optimal solutions computed from biomechanical models is not known. Here, we examined the range of biomechanically permitted activation levels in individual muscles during human walking using a detailed musculoskeletal model and experimentally-measured kinetics and kinematics. Feasible muscle activation ranges define the minimum and maximum possible level of each muscle's activation that satisfy inverse dynamics joint torques assuming that all other muscles can vary their activation as needed. During walking, 73% of the muscles had feasible muscle activation ranges that were greater than 95% of the total muscle activation range over more than 95% of the gait cycle, indicating that, individually, most muscles could be fully active or fully inactive while still satisfying inverse dynamics joint torques. Moreover, the shapes of the feasible muscle activation ranges did not resemble previously-reported muscle activation patterns nor optimal solutions, i.e. static optimization and computed muscle control, that are based on the same biomechanical constraints. Our results demonstrate that joint torque requirements from standard inverse dynamics calculations are insufficient to define the activation of individual muscles during walking in healthy individuals. Identifying feasible muscle activation ranges may be an effective way to evaluate the impact of additional biomechanical and/or neural constraints on possible versus actual muscle activity in both normal and impaired movements.

1. Introduction

Musculoskeletal redundancy (Bernstein, 1967) allows for an infinite number of combinations of muscle activation patterns for performing a task. Current modeling approaches typically handle this redundancy by assuming some optimization criterion, e.g. minimizing muscle stress (Crowninshield and Brand, 1981; Thelen et al., 2003), to select a single muscle activation pattern among many that satisfy biomechanical constraints such as joint torques, joint contact forces (Fregly et al., 2012; Lin et al., 2010; Walter et al., 2014), joint impedance (Franklin and Wolpert, 2011; Hogan, 1984; Mitrovic et al., 2010), etc. The most common biomechanical constraints on muscle activation patterns are based on experimentally-measured kinematics (e.g. joint angles) and kinetics (e.g. ground reaction forces) and found using a single optimization criterion. Such inverse approaches identify optimal solutions that may capture major features of experimentally-measured muscle activation patterns (Thelen and Anderson, 2006; Thelen et al., 2003), but do not inform the extent to which deviations from optimal patterns may also satisfy the biomechanical constraints. While some variations in muscle activity across individuals have been attributed to different body morphology (Buchanan and Shreeve, 1996; Liu et al., 2008; van der Krogt et al., 2012), how much within-individual variations of muscle activity are permitted given these biomechanical constraints has not been well studied. Characterizing all viable deviations in muscle activity from an optimal solution that still satisfy a set of biomechanical constraints would facilitate interpretation of experimental variations in muscle activation patterns as well as how those biomechanical constraints affect not just the optimal solutions, but the set of all possible solutions.

A few attempts to define feasible muscle activation ranges for a given movement have been made previously. These attempts have been limited to matching net joint torques, primarily in isometric tasks, and their results may be highly dependent on model complexity. For example, Kutch and Valero-Cuevas (2011; 2012) demonstrated a limited range of possible muscle activation patterns for finger forces in a 4 degree-of-freedom (DoF) model with 7 muscles, suggesting that biomechanics limit the set of possible muscle activation patterns. Using a simplified planar leg model with 14

* Corresponding author: 313 Ferst Drive, Atlanta, GA 30332-0535, United States Tel. 404 894 5216, fax: 404 385 5044
E-mail address: lting@emory.edu (L.H. Ting).

http://dx.doi.org/10.1016/j.jbiomech.2015.07.037
0021-9290/

muscles and three DoFs, they demonstrated using computational geometry that removing a single muscle greatly reduces force production capabilities; this approach defines the complete solution space but is limited to 14 muscles. In contrast, we demonstrated very wide feasible muscle activation ranges using a linear programming technique on a model of the cat hindlimb with 7 DoFs and 41 muscles (Sohn et al., 2013). Similarly, Martelli et al. showed wide possible variations in a model of human walking (10 DoFs, 82 muscles), however the Markov Chain Monte Carlo methods they used cannot find explicit limits of activation (Martelli et al., 2015, 2013).

Here, our goal was to identify the feasible muscle activation ranges during a full gait cycle of human walking by extending the methods of Sohn et al. (2013) to a dynamic task. We identified feasible muscle activation ranges during human walking using experimental data (John et al., 2013) and a detailed musculoskeletal model of the human lower extremity with 23 DoF and 92 muscles (Delp et al., 2007; Delp et al., 1990). We extended Sohn's (2013) method such that each time point in the gait cycle was treated as an independent optimization problem (Anderson and Pandy, 2001b), where each muscle's minimum and maximum possible activity level (while allowing all others to vary independently) to satisfy inverse dynamics based net joint torque requirements is identified at each time point. These upper and lower bounds on muscle activation, defining the feasible muscle activation ranges, were then compared to optimal solutions from inverse approaches, i.e., computed muscle control (CMC) (Thelen and Anderson, 2006; Thelen et al., 2003) and static optimization (Anderson and Pandy, 2001b) as well as experimentally recorded electromyographic (EMG) data reported in literature (Perry, 1992; Van der Krogt et al., 2012). Our results show that feasible muscle activation ranges can be applied to standard inverse dynamics solutions using complex musculoskeletal models to identify the degree to which muscle activation level can vary from optimal solutions.

2. Methods

Our method for calculating feasible muscle activation ranges was based on satisfying inverse dynamics joint torque constraints and used a combination of built-in OpenSim analyses with custom Matlab code (Fig. 1). Experimental data in combination with a generic OpenSim model (Scale, Inverse Kinematics, and Inverse Dynamics Tools) were used to calculate movement kinematics and kinetics. Joint torques and muscle parameters extracted from the model were used as inputs to calculate feasible ranges of muscle activation. Our results were compared to solutions from commonly used techniques to calculate optimal muscle activations, specifically static optimization (Anderson and Pandy, 2001b) and CMC (Thelen and Anderson, 2006). We also compared our feasible muscle activation ranges to EMG data from Perry (1992) and van der Krogt et al. (2012).

2.1. Experimental data

We used experimental marker data and ground reaction force data (Fig. 1) of a single subject (male; height, 1.83 m; body mass, 65.9 kg) walking at self-selected speed (1.36 m/s) on an instrumented treadmill. This data is publically available at https://simtk.org/home/muscleprops (John et al., 2013).

2.2. Extraction of model parameters from OpenSim

A generic three-dimensional OpenSim musculoskeletal model of the human lower extremity (gait2392.osim) with 23 DoF and 92 musculotendon actuators (Table 1) was scaled to subject anthropometrics using the Scale Tool. The muscle model parameters extracted for each muscle were: maximum isometric force, optimal fiber length, tendon slack length, pennation angle at optimal fiber length, maximum eccentric force, parallel muscle fiber stiffness, active force-length, passive force-length, and force-velocity shape factors. Joint angles were calculated using the Inverse Kinematics Tool with the scaled model and experimental marker data. Musculotendon lengths and moment arms were extracted from inverse kinematics results. Finally, joint torques were calculated using the Inverse Dynamics Tool with the scaled model, inverse kinematics results, and experimental ground reaction forces.

2.3. Calculating feasible muscle activation ranges

Feasible muscle activation ranges were calculated using custom Matlab code based on a linear mapping between muscle activations ($\bar{a}$) and the joint torques ($\bar{\tau}$) required to produce the task calculated using OpenSim (above):

$$\boldsymbol{R}[\bar{q}(T)]\bullet\boldsymbol{AMF}[\bar{q}(T),\dot{\bar{q}}(T)]\bullet\bar{a}(T)=\bar{\tau}(\mathrm{T})-\boldsymbol{R}[\bar{q}(T)]\bullet\boldsymbol{PMF}[\bar{q}(T)]$$

where $\boldsymbol{R}$ is the moment arm matrix dependent on joint angle, $\boldsymbol{AMF}$ is the active muscle force contribution, and $\boldsymbol{PMF}$ is the passive muscle force contribution. Both $\boldsymbol{AMF}$ and $\boldsymbol{PMF}$ were computed according to force-length and force-velocity relationships in a Hill-type muscle model (Thelen, 2003) from John et al. (2013). Tendons were assumed to be inelastic (Zajac and Gordon, 1989).

Feasible muscle activation ranges were computed for each muscle at each time point for one complete gait cycle (1.2 s at 72 Hz) and define the upper and lower bounds of each muscle's activation while allowing all other muscles to vary independently. The upper and lower bounds were found using linear programming (linprog.m in Matlab). For each muscle and each time point, the lower (a_M^{LB}) and upper (a_M^{UB}) bounds of muscle activation were identified as follows (Sohn et al., 2013):

a_M^{LB}: Find a^m such that $|\bar{a}|$ is minimized, while

$$\boldsymbol{R}[\bar{q}(T)]\bullet\boldsymbol{AMF}[\bar{q}(T),\dot{\bar{q}}(T)]\bullet\bar{a}(T)=\bar{\tau}(\mathrm{T})-\boldsymbol{R}[\bar{q}(T)]\bullet\boldsymbol{PMF}[\bar{q}(T)]$$

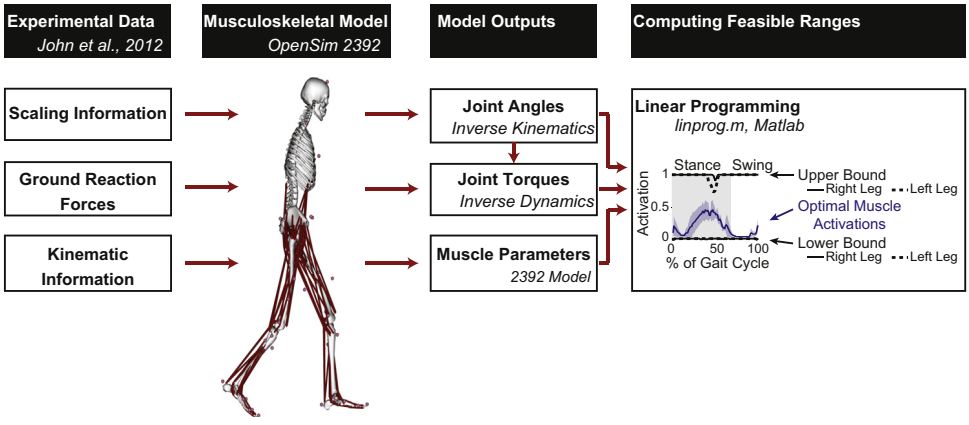

Fig. 1. Schematic of methods used to identify feasible ranges of muscle activation during walking. An OpenSim human lower limb musculoskeletal model with 23 degrees of freedom and 92 muscles (Delp et al. 1990, 2007) was used to perform an inverse dynamics analysis of experimental data from John et al. (2013). Native OpenSim tools (Inverse Kinematics and Inverse Dynamics) were used to calculate joint angles and torques as well as to extract muscle properties necessary to compute muscle force production capabilities (Thelen, 2003; John et al., 2013). Feasible muscle activation ranges were then computed using linear programming (linprog.m) in Matlab. Feasible muscle activation ranges can be compared with optimal or experimental (EMG) muscle activations by superimposing muscle activations onto the feasible ranges.

Table 1
Muscles included in the OpenSim 2392 musculoskeletal model and their abbreviations.

Name	Abbreviation	Name	Abbreviation
Adductor brevis	ADB	*Peroneus brevis*	PB
Adductor longus	ADL	*Peroneus longus*	PL
Adductor magnus	ADM	*Peroneus tertius*	PT
Biceps femoris long head	BFLH	*Piriformis*	PIR
Biceps femoris short head	BFSH	*Iliopsoas*	PSOAS
Extensor digitorum	ED	*Quadratus femoris*	QF
Extensor hallucis	EH	*Rectus femoris*	RF
Flexor digitorum	FD	*Sartorius*	SAR
Flexor hallicus	FH	*Semimembranossus*	SM
Gemellus	GEM	*Soleus*	SOL
Gluteus maximus	GMAX	*Semitendinosus*	ST
Gluteus medius	GMED	*Tibialis anterior*	TA
Gluteus minimus	GMIN	*Tibialis posterior*	TP
Gracilis	GRAC	*Tensor fasciae latae*	TFL
Illiacus	ILI	*Vastus intermedius*	VI
Lateral gastrocnemius	LG	*Vastus lateralis*	VL
Medial gastrocnemius	MG	*Vastus medialis*	VM
Pectineus	PEC		

a_M^{UB}: Find a^m such that $|\bar{a}|$ is maximized, while

$$\boldsymbol{R}[\bar{q}(T)]\cdot\boldsymbol{AMF}[\bar{q}(T),\dot{\bar{q}}(T)]\cdot\bar{a}(T)=\bar{\tau}(T)-\boldsymbol{R}[\bar{q}(T)]\cdot\boldsymbol{PMF}\bar{q}(T)$$

while satisfying the constraint: $0\le a^m\le 1$. We examined the feasible muscle activation ranges for 86 leg muscles.

2.4. Comparison to optimal muscle activation patterns

We compared feasible muscle activation ranges to optimal muscle activations based on measured kinetics and kinematics using:

1. Static optimization: Optimal muscle activations based on minimizing $\bar{a}^T\bar{a}$ were found using quadratic programming in Matlab (quadprog.m).
2. Computed Muscle Control (CMC): Optimal muscle activations from CMC (Thelen and Anderson, 2006; Thelen et al., 2003) were found using the OpenSim CMC tool with settings provided by John et al. (2013).

Both techniques use a cost function that minimizes the sum of squared muscle activations (Crowninshield and Brand, 1981). However, CMC explicitly accounts for delays in muscle force production due to muscle activation and musculotendon contraction dynamics, while static optimization does not.

2.5. Comparison to experimental muscle activity

We compared feasible muscle activation ranges to observed muscle activity previously recorded by others. First, we identified time-points when each muscle is typically "active" versus "inactive" based on previously published timing of muscle activity during human walking (Perry, 1992). We then compared whether the value of each muscle's upper bound was different when the muscle is typically active versus inactive using single-tailed two-sample *t*-tests with 95% confidence levels.

We overlaid EMG signals from six muscles to qualitatively compare feasible muscle activation ranges defined by joint torques to experimental muscle activity patterns. Since EMG data was not available for the subject from whom the kinetic, kinematic, and scaling data came (John et al., 2013), EMG data (scaled to the peak optimal muscle activations from CMC (Thelen and Anderson, 2006)) from van der Krogt et al. (2012) were used. Data from van der Krogt et al. (2012) were presented as average $\pm$ standard deviation over 5 healthy subjects (16 ± 1 years; 68 ± 5 kg; 175 ± 9 cm height) walking at self-selected speed 1.08 ± 0.06 m/s.

3. Results

3.1. Feasible muscle activation ranges

Feasible activation ranges for individual muscles were largely unconstrained during walking based on inverse dynamics joint torques (Fig. 3) where each muscle's feasible activation range was computed independently, allowing all other muscle activations to vary as necessary. Seventy-three percent (63/86) of muscles had fully unconstrained feasible muscle activation ranges with upper bounds of 1 and lower bounds of 0 over the entire gait cycle. Feasible muscle activation ranges in the right leg were slightly larger than those of the left leg due to differences in kinematics and kinetics (Fig. 2).

Almost no muscles were "necessary", defined as having non-zero lower bounds (Fig. 3, black lower traces). All muscles in the right leg had a lower bound of zero throughout the gait cycle (Fig. 3, solid black lower traces). Only two left-leg muscles, the tibialis anterior (TA) and the anterior compartment of gluteus medius (GMED1), had non-zero lower bounds at some point during the gait cycle (Fig. 3, dotted black lower traces). The left TA lower bound increased above zero in early stance, consistent with controlling the descent of the toe. The left GMED1 was necessary in late stance, where hip abduction torque was larger in the left versus right leg (Fig. 2C, black dotted versus solid line). However, GMED has not typically been reported to be active (Fig. 3, orange lines) in late stance.

Overall, 73% (63 out of 86) of muscles were "unlimited" in their feasible level of activity, defined as having an upper bound of 1 at every time point in the gait cycle (Fig. 3, black upper traces). Several muscles about the hip were limited in their upper bounds in late stance, e.g. gluteus maximus (GMAX) and gluteus medius (GMED), but never in swing phase. Several ankle plantarflexors, e.g. medial gastrocnemius (MG) and lateral gastrocnemius (LG), were constrained in early stance and late swing phase. The soleus (SOL), the strongest muscle in the model, was the most limited muscle.

3.2. Comparison to optimal muscle activation patterns

Different optimal muscle activation patterns were found using static optimization and CMC (Fig. 3, blue and green traces). CMC solutions required all muscles to be active at some point during the gait cycle. In contrast, static optimization activated fewer muscles, with about 46% (20 of 43) silent throughout the gait cycle, requiring larger activation of some muscles compared to CMC (e.g. GMAX2 and VI). Despite these differences, the solutions from both methods for almost all muscles fell within the feasible muscle activation ranges (Fig. 3, compare blue and black traces). One muscle in the CMC solution, right soleus, exceeded the upper bound of the feasible muscle activation range due to the activity of reserve actuators used in CMC. Finally, optimal muscle activations for some plantarflexor muscles (SOL and MG) appear to be lower when the corresponding upper bounds of feasible activation are constrained (less than one, Fig. 3).

3.3. Comparison to experimental muscle activity

Overall, 44% (8 out of 18) of "limited" muscles, defined as having upper bound of less than 1 at some point during the gait cycle, had smaller upper bounds at time points when the muscle is typically inactive during gait, and higher upper bounds when the muscle is typically active during gait. For example, upper bounds on GMED3 were higher in early stance where it is typically active (Fig. 3, orange bars) compared to late stance where it is typically inactive. Only 11% (2 out of 18, left LG and left ADL) of "limited" muscles showed the opposite pattern in which upper bounds were smaller when they are typically active compared to when they are typically inactive. Finally, variability in the sample experimental EMG data was much smaller than the feasible muscle activation ranges (Fig. 4).

4. Discussion

Our results demonstrate joint torque requirements from standard inverse dynamics analysis are not sufficient to define the activation level of individual muscles during walking in healthy

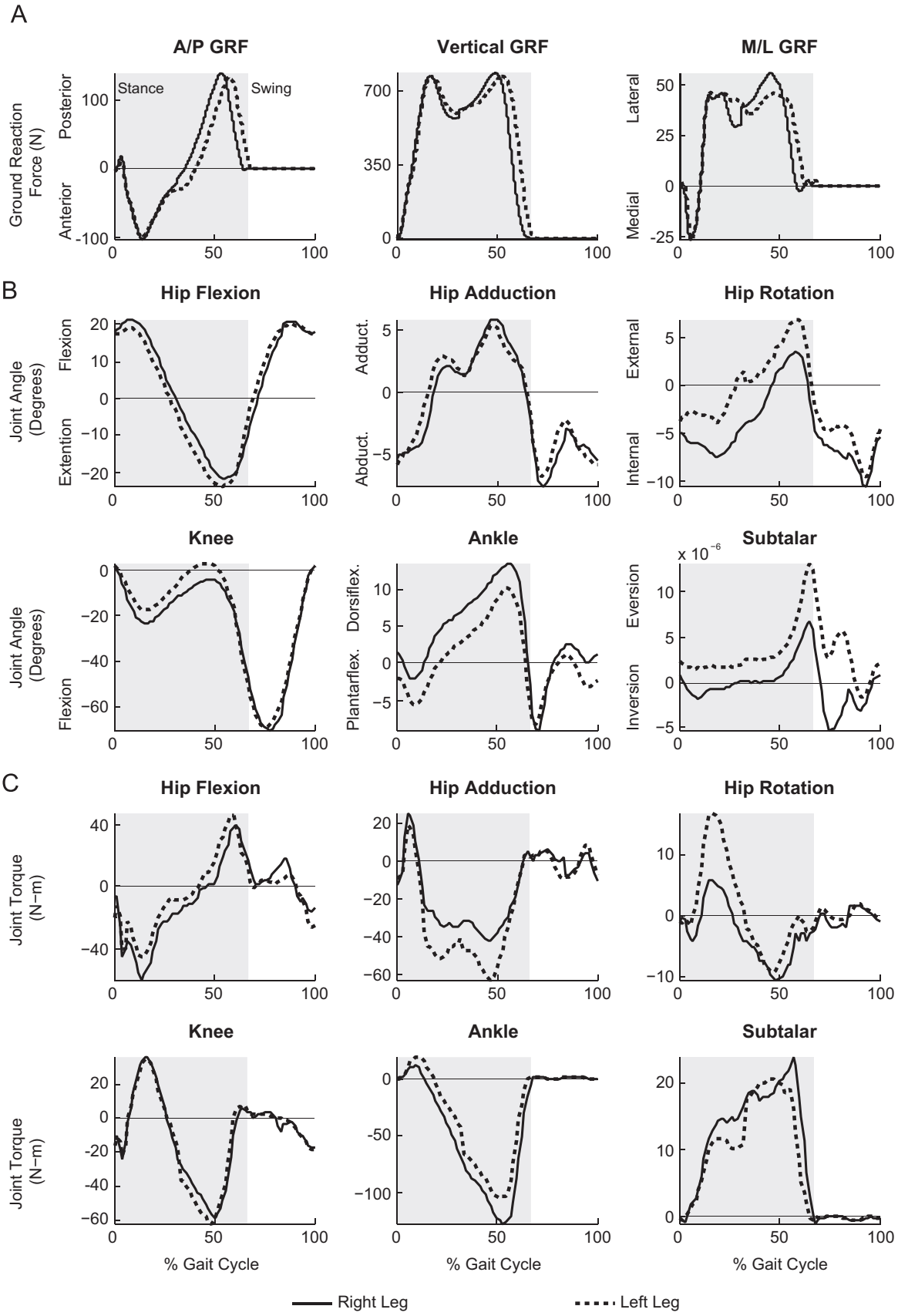

Fig. 2. Experimental data used for computing feasible ranges during walking. (A) Ground reaction forces data for one gait cycle taken from John et al. (2013) and available on www.simtk.org. The shaded grey region indicates the stance phase of the gait cycle. (B) Joint angles computed using the Inverse Kinematics Tool in OpenSim using marker data from John et al. (2013). Joint angles were used for computing kinematic properties of muscles, i.e. force–length and force–velocity relationships. (C) Joint torques computed using the Inverse Dynamics Tool in OpenSim with the ground reaction forces shown in A and the joint angles shown in B. These joint torques were used as task requirements for which feasible muscle activation ranges were identified.

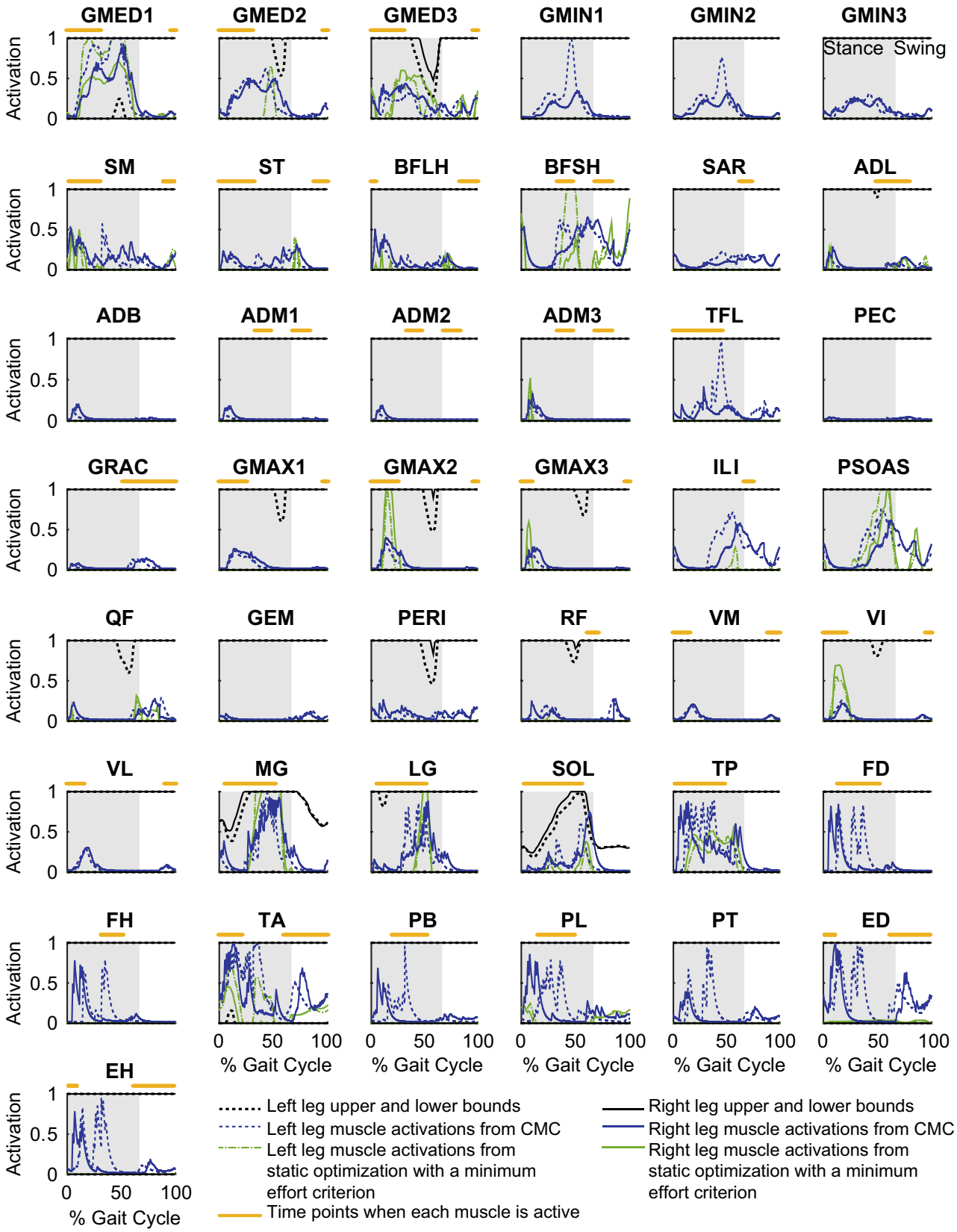

Fig. 3. Feasible muscle activation ranges over one gait cycle and optimal muscle activations from static optimization and CMC. Orange lines indicate when muscles are typically active during gait based on normative data (Perry, 1992). The shaded grey region indicates the stance phase of the gait cycle. Feasible muscle activation ranges for each muscle are defined by all activation levels bounded by the upper and lower bounds of muscle activity (black lines). Feasible muscle activation ranges were generally very wide, showing that each individual muscle's activation is virtually unconstrained based on joint torques if all other muscles can vary independently to satisfy joint torque requirements. Optimal muscle activations computed using quadratic programming (quadprog.m) in MATLAB with a minimum effort criteria (green) and using computed muscle control (CMC, blue) fall within the feasible muscle activation ranges. (For interpretation of the references to color in this figure legend,the reader is referred to the web version of this article.)

individuals. Based on torque-producing properties of muscles (moment arms, force–length and force-velocity relationships) and joint torque requirements across the entire gait cycle, we identified feasible muscle activation ranges that define the upper and lower bounds on muscle activation levels (Sohn et al., 2013; Valero-Cuevas et al., 2015) from which a particular solution may be selected for a task. The largely unconstrained feasible muscle activation ranges reflect a large degree of musculoskeletal redundancy in human walking, allowing a wide range of deviations from optimal muscle activation patterns in the activation of any individual muscle while satisfying joint torque requirements. Variability in experimental muscle activation patterns appear to be much more restricted than the feasible muscle activation ranges. In the future, feasible muscle activation ranges may be a useful tool for examining the effects of model complexity as well as additional biomechanical or neural constraints on the set of possible muscle activation patterns for gait and other movements.

We found virtually no limitations on activation of individual muscles during walking, suggesting a great deal of robustness to deviations in motor patterns from optimal solutions identified using inverse approaches. The general shape and features of optimal solutions were not evident in the wide feasible muscle activation ranges (Crowninshield and Brand, 1981; Thelen and Anderson, 2006; Thelen et al., 2003). The zero-valued lower bounds found in virtually all muscles shows that almost any individual muscle can be completely silenced in walking without reducing the ability to meet the joint torque demands. Accordingly, simulations of healthy subjects in normal gait show surprising robustness to muscle weakness (van der Krogt et al., 2012). In contrast, prior experiments on cadaveric human hands and a simplified leg model have demonstrated limited robustness to muscle dysfunction that suggests very little musculoskeletal redundancy (Kutch and Valero-Cuevas, 2011; Valero-Cuevas and Hentz, 2002); a primary difference is the relatively large number of muscles we used (43 per leg) compared to those studies. It is likely that feasible muscle activation ranges are wide at self-selected walking speed because it is a relatively easy task for the human leg compared

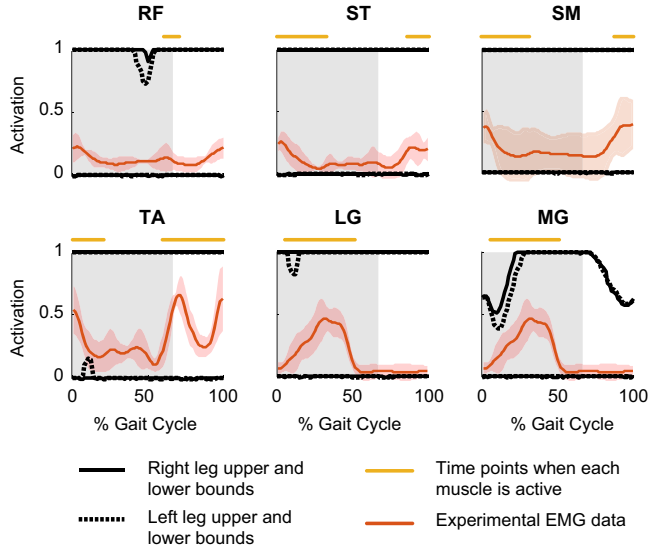

Fig. 4. Feasible muscle activation ranges superimposed on experimental EMG data and CMC muscle activations. Feasible muscle activation ranges defined by upper and lower bounds of muscle activation are shown as black traces. Orange lines indicate when muscles are known to be active during gait from normative data (Perry, 1992). The shaded grey region indicates the stance phase of the gait cycle. Red lines and shading show experimental EMG data (mean and standard error) from 5 subjects during self-selected walking speed (van der Krogt et al., 2012). (For interpretation of the references to color in this figure legend,the reader is referred to the web version of this article.)

more demanding tasks such as jumping or sprinting, where feasible muscle activation ranges are likely more restricted.

Examining the further restriction of feasible muscle activation ranges based on additional biomechanical and/or neural constraints may be an effective way to evaluate the impact of other physiological considerations on muscle activity. Here, as proof of concept, we considered only the minimal set of biomechanical constraints used in a standard inverse dynamics approach, based primarily on net joint torque requirements and muscle properties. Other biomechanical constraints not considered in this study may potentially affect the results. For example, including compliant tendons and ligaments may increase feasible muscle activation ranges. While evidence suggests this would not greatly alter analysis of walking (Arnold and Delp, 2011; Arnold et al., 2013), more dynamic tasks such as running or jumping may be more affected. Consideration of joint mobility or physiological joint contact forces may provide further constraints and decrease feasible muscle activation ranges. It is likely that an interplay of both neural and biomechanical constraints determines muscle activation patterns (Fregly et al., 2012; Lin et al., 2010; Walter et al., 2014). Feasible muscle activation ranges can be a useful tool for investigating how various constraints affect possible variations in muscle activity.

The linear programming method used here to find feasible muscle activation ranges can be applied to musculoskeletal models of any level of complexity and identify explicit bounds on the activity of single muscles; however, it does not identify multi-muscle activation patterns for a given movement. The primary contribution of this work was to extend methods developed by Sohn et al. (2013) for static force production to a dynamic task by including inertial and velocity-dependent forces in the equations of motion. While we did not account for muscle activation dynamics, e.g. timing of fiber-type differences, prior work has demonstrated that independent static optimization at each time point can produce similar results to dynamic optimization in sub-maximal tasks such as human walking (Anderson and Pandy, 2001b). Our method, based on linear programming, can be applied to models of any complexity whereas computational geometry algorithms (Kutch and Valero-Cuevas 2011; 2012) can only be applied to systems that have a relatively low number (<14 of muscles). One advantage of the computational geometry approach is that the entire solution space is defined, allowing correlations across multiple muscles that are imposed by task constraints to be identified. In contrast, our bounds represent only the extreme points on the solution space for each muscle considered independently. However, further analysis using feasible muscle activation ranges may be possible to reveal explicit relationships between muscles for satisfying joint torques. In contrast to the stochastic search methods of Martelli et al. (2015; 2013) that do not guarantee identification of the true bounds of the solution space even when a large number of samples (e.g. 200,000) is used, our linear programming methods finds explicit upper and lower bounds for each muscle independently. Our results are similar to those of Martelli et al. (2015), except that their method constrained certain muscles to adhere to measured EMG levels, defining plausible muscle force patterns in the muscles that were not measured. Similar constraints can easily be implemented in the methods presented here.

A limitation of all of the methods used to identify feasible muscle activation ranges is that only specified movements can be analyzed. Thus the effect of removing a muscle on changes in movement dynamics cannot be found, yet changes in movement dynamics would likely result from removing or weakening a muscle. Optimal control models that simulate human walking (Ackermann and van den Bogert, 2010; Anderson and Pandy, 2001a) could be used to identify changes in the dynamics of walking due to muscle weakness, but also rely on an objective function to identify a single muscle activation pattern from among many possible. Considerable advances

in computational methods are necessary to combine feasible ranges of muscle activation analyses with dynamic optimization to predict movement patterns. However, it is likely that even more latitude in muscle activation patterns would be revealed using optimal control methods due to the ability of the model to select dynamics most suitable to its force producing capabilities instead of having to replicate a specified motion.

Nevertheless, feasible muscle activation ranges may be useful for investigating how muscle activation patterns are influenced by various biomechanical and/or neural constraints, including clinical impairments. For example, the lower bound shows the minimum activation, and by extension, the minimum strength permissible for each individual muscle to perform a movement. Other studies using similar models and constraints have examined musculoskeletal redundancy using trial and error methods of weakening or eliminating muscles or muscle groups to show whether deficits in task performance occur (Arnold et al., 2005; Correa et al., 2012; Hicks et al., 2008; Steele et al., 2012). These studies use computed muscle control (CMC) (Thelen and Anderson, 2006; Thelen et al., 2003) to identify optimal compensation for muscle weakness, whereas feasible muscle activation ranges can identify the set of possible compensations. Although we did not include neural constraints in our analysis, feasible ranges of muscle activations could be further narrowed by including neurally-inspired constraints that constrain the timing or recruitment of multiple muscles (Ivanenko et al., 2004; Ting and Macpherson, 2005), impose multiple task constraints (Keenan et al., 2009; Racz et al., 2012), or include stability considerations (Bunderson et al., 2008). Feasible muscle activation ranges may also be useful for understanding the impact of neuromuscular impairments such as stroke (Dewald et al., 1995; McCrea et al., 2005), spinal-cord injury (Chvatal et al., 2013; Hayes et al., 2014), or limb loss (Prinsen et al., 2011; Soares et al., 2009; Vrieling et al., 2008; Waters and Mulroy, 1999). Understanding actual versus possible variations in muscle activity using feasible muscle activation ranges may provide an important foundation in understanding both healthy and impaired motor control.

Conflict of interest statement

The authors declare that they have no conflicts of interest.

Acknowledgments

Air Products Undergraduate Research Award to CSS and NIH grant HD46922 to LHT. JLA was supported by NIH T32 NS007480. Air Products and NIH had no role in the design, performance, or interpretation of the study.

References

Ackermann, M., van den Bogert, A.J., 2010. Optimality principles for model-based prediction of human gait. J. Biomech. 43, 1055–1060.
Anderson, F.C., Pandy, M.G., 2001a. Dynamic optimization of human walking. J. Biomech. Eng. 123, 381–390.
Anderson, F.C., Pandy, M.G., 2001b. Static and dynamic optimization solutions for gait are practically equivalent. J. Biomech. 34, 153–161.
Arnold, A.S., Anderson, F.C., Pandy, M.G., Delp, S.L., 2005. Muscular contributions to hip and knee extension during the single limb stance phase of normal gait: a framework for investigating the causes of crouch gait. J. Biomech. 38, 2181–2189.
Arnold, E.M., Delp, S.L., 2011. Fibre operating lengths of human lower limb muscles during walking. Philos. Trans. R. Soc. Lond. B: Biol. Sci. 366, 1530–1539.
Arnold, E.M., Hamner, S.R., Seth, A., Millard, M., Delp, S.L., 2013. How muscle fiber lengths and velocities affect muscle force generation as humans walk and run at different speeds. J. Exp. Biol. 216, 2150–2160.
Bernstein, N., 1967. The Coordination and Regulation of Movements. Pergamon Press, New York.
Buchanan, T.S., Shreeve, D.A., 1996. An evaluation of optimization techniques for the prediction of muscle activation patterns during isometric tasks. J. Biomech. Eng. 118, 565–574.
Bunderson, N.E., Burkholder, T.J., Ting, L.H., 2008. Reduction of neuromuscular redundancy for postural force generation using an intrinsic stability criterion. J. Biomech.
Chvatal, S.A., Macpherson, J.M., Torres-Oviedo, G., Ting, L.H., 2013. Absence of postural muscle synergies for balance after spinal cord transection. J. Neurophysiol. 110, 1301–1310.
Correa, T.A., Schache, A.G., Graham, H.K., Baker, R., Thomason, P., Pandy, M.G., 2012. Potential of lower-limb muscles to accelerate the body during cerebral palsy gait. Gait Posture 36, 194–200.
Crowninshield, R.D., Brand, R.A., 1981. A physiologically based criterion of muscle force prediction in locomotion. J. Biomech. 14, 793–801.
Delp, S.L., Anderson, F.C., Arnold, A.S., Loan, P., Habib, A., John, C.T., Guendelman, E., Thelen, D.G., 2007. OpenSim: open-source software to create and analyze dynamic simulations of movement. IEEE Trans. Bio-Med. Eng. 54, 1940–1950.
Delp, S.L., Loan, J.P., Hoy, M.G., Zajac, F.E., Topp, E.L., Rosen, J.M., 1990. An interactive graphics-based model of the lower extremity to study orthopaedic surgical procedures. IEEE Trans. Bio-Medical Eng. 37, 757–767.
Dewald, J.P., Pope, P.S., Given, J.D., Buchanan, T.S., Rymer, W.Z., 1995. Abnormal muscle coactivation patterns during isometric torque generation at the elbow and shoulder in hemiparetic subjects. Brain 118 (Pt 2), 495–510.
Franklin, D.W., Wolpert, D.M., 2011. Computational mechanisms of sensorimotor control. Neuron 72, 425–442.
Fregly, B.J., Besier, T.F., Lloyd, D.G., Delp, S.L., Banks, S.A., Pandy, M.G., D'Lima, D.D., 2012. Grand challenge competition to predict in vivo knee loads. J. Orthop. Res. 30, 503–513.
Hayes, H.B., Chvatal, S.A., French, M.A., Ting, L.H., Trumbower, R.D., 2014. Neuromuscular constraints on muscle coordination during overground walking in persons with chronic incomplete spinal cord injury. Clin. Neurophysiol.: Off. J. Int. Fed. Clin. Neurophysiol. 125, 2024–2035.
Hicks, J.L., Schwartz, M.H., Arnold, A.S., Delp, S.L., 2008. Crouched postures reduce the capacity of muscles to extend the hip and knee during the single-limb stance phase of gait. J. Biomech. 41, 960–967.
Hogan, N., 1984. Adaptive control of mechanical impedance by coactivation of antagonist muscles. IEEE Trans. Autom. Control 29, 681–690.
Ivanenko, Y.P., Poppele, R.E., Lacquaniti, F., 2004. Five basic muscle activation patterns account for muscle activity during human locomotion. J. Physiol. 556, 267–282.
John, C.T., Anderson, F.C., Higginson, J.S., Delp, S.L., 2013. Stabilisation of walking by intrinsic muscle properties revealed in a three-dimensional muscle-driven simulation. Comput. Methods Biomech. Biomed. Eng. 16, 451–462.
Keenan, K.G., Santos, V.J., Venkadesan, M., Valero-Cuevas, F.J., 2009. Maximal voluntary fingertip force production is not limited by movement speed in combined motion and force tasks. J. Neurosci.: Off. J. Soc. Neurosci. 29, 8784–8789.
Kutch, J.J., Valero-Cuevas, F.J., 2011. Muscle redundancy does not imply robustness to muscle dysfunction. J. Biomech. 44, 1264–1270.
Kutch, J.J., Valero-Cuevas, F.J., 2012. Challenges and new approaches to proving the existence of muscle synergies of neural origin. PLoS Comput. Biol. 8, e1002434.
Lin, Y.C., Walter, J.P., Banks, S.A., Pandy, M.G., Fregly, B.J., 2010. Simultaneous prediction of muscle and contact forces in the knee during gait. J. Biomech. 43, 945–952.
Liu, M.Q., Anderson, F.C., Schwartz, M.H., Delp, S.L., 2008. Muscle contributions to support and progression over a range of walking speeds. J. Biomech. 41, 3243–3252.
Martelli, S., Calvetti, D., Somersalo, E., Viceconti, M., 2015. Stochastic modelling of muscle recruitment during activity. Interface Focus 5, 20140094.
Martelli, S., Calvetti, D., Somersalo, E., Viceconti, M., Taddei, F., 2013. Computational tools for calculating alternative muscle force patterns during motion: a comparison of possible solutions. J. Biomech. 46, 2097–2100.
McCrea, P.H., Eng, J.J., Hodgson, A.J., 2005. Saturated muscle activation contributes to compensatory reaching strategies after stroke. J. Neurophysiol. 94, 2999–3008.
Mitrovic, D., Klanke, S., Osu, R., Kawato, M., Vijayakumar, S., 2010. A computational model of limb impedance control based on principles of internal model uncertainty. PloS One 5, e13601.
Perry, J., 1992. Gait Analysis: Normal and Pathological Function. Thorofare, NJ.
Prinsen, E.C., Nederhand, M.J., Rietman, J.S., 2011. Adaptation strategies of the lower extremities of patients with a transtibial or transfemoral amputation during level walking: a systematic review. Arch. Phys. Med. Rehabil. 92, 1311–1325.
Racz, K., Brown, D., Valero-Cuevas, F.J., 2012. An involuntary stereotypical grasp tendency pervades voluntary dynamic multifinger manipulation. J. Neurophysiol. 108, 2896–2911.
Soares, A.S., Yamaguti, E.Y., Mochizuki, L., Amadio, A.C., Serrao, J.C., 2009. Biomechanical parameters of gait among transtibial amputees: a review. Sao Paulo Med. J.=Rev. Paul. De Med. 127, 302–309.
Sohn, M.H., McKay, J.L., Ting, L.H., 2013. Defining feasible bounds on muscle activation in a redundant biomechanical task: practical implications of redundancy. J. Biomech. 46, 1363–1368.
Steele, K.M., van der Krogt, M.M., Schwartz, M.H., Delp, S.L., 2012. How much muscle strength is required to walk in a crouch gait? J. Biomech. 45, 2564–2569.

Thelen, D.G., 2003. Adjustment of muscle mechanics model parameters to simulate dynamic contractions in older adults. J. Biomech. Eng. 125, 70–77.
Thelen, D.G., Anderson, F.C., 2006. Using computed muscle control to generate forward dynamic simulations of human walking from experimental data. J. Biomech. 39, 1107–1115.
Thelen, D.G., Anderson, F.C., Delp, S.L., 2003. Generating dynamic simulations of movement using computed muscle control. J. Biomech. 36, 321–328.
Ting, L.H., Macpherson, J.M., 2005. A limited set of muscle synergies for force control during a postural task. J. Neurophysiol. 93, 609–613.
Valero-Cuevas, F.J., Cohn, B.A., Yngvason, H.F., Lawrence, E.L., 2015. Exploring the high-dimensional structure of muscle redundancy via subject-specific and generic musculoskeletal models. J. Biomech.
Valero-Cuevas, F.J., Hentz, V.R., 2002. Releasing the A3 pulley and leaving flexor superficialis intact increases pinch force following the Zancolli lasso procedures to prevent claw deformity in the intrinsic palsied finger. J. Orthop. Res. 20, 902–909.
van der Krogt, M.M., Delp, S.L., Schwartz, M.H., 2012. How robust is human gait to muscle weakness? Gait Posture 36, 113–119.
Vrieling, A.H., van Keeken, H.G., Schoppen, T., Otten, E., Hof, A.L., Halbertsma, J.P., Postema, K., 2008. Balance control on a moving platform in unilateral lower limb amputees. Gait Posture 28, 222–228.
Walter, J.P., Kinney, A.L., Banks, S.A., D'Lima, D.D., Besier, T.F., Lloyd, D.G., Fregly, B.J., 2014. Muscle synergies may improve optimization prediction of knee contact forces during walking. J. Biomech. Eng. 136, 021031.
Waters, R.L., Mulroy, S., 1999. The energy expenditure of normal and pathologic gait. Gait Posture 9, 207–231.
Zajac, F.E., Gordon, M.E., 1989. Determining muscle's force and action in multi-articular movement. Exerc. Sport Sci. Rev. 17, 187–230.